CHEMMEDCHEM

CHEMISTRY ENABLING DRUG DISCOVERY

Accepted Article

Title: Binding and release of Fe(III) complexes from glucan particles for delivery of T1 MRI contrast agents

Authors: Akanksha Patel, Didar Asik, Eric M Snyder, Alexandra E Delillo, Paul J Cullen, and Janet Ruth Morrow

To be cited as: *ChemMedChem* 10.1002/cmdc.202000003

Link to VoR: http://dx.doi.org/10.1002/cmdc.202000003

A Journal of

ChemPubSoc Europe

WILEY-VCH

www.chemmedchem.org

WILEY-VCH

FULL PAPER

Binding and release of Fe(III) complexes from glucan particles for delivery of T_1 MRI contrast agents.

Akanksha Patel,[a] Didar Asik,[a] Eric M. Snyder,[a] Alexandra E. Dilillo,[a] Paul J. Cullen,[b] and Janet R. Morrow[a*]

[a] Dr. J. R. Morrow, A. Patel, D. Asik, E. M. Snyder, A. E. Dilillo
Department of Chemistry
University at Buffalo
State University of New York, Amherst, NY 14260
E-mail: jmorrow@buffalo.edu
[b] P. J. Cullen
Department of Biology
University at Buffalo
State University of New York, Amherst, NY 14260

Supporting information for this article is given via a link at the end of the document

Abstract: Yeast derived β-glucan particles (GPs) are a class of microcarriers under development for the delivery of drugs and imaging agents to immune system cells for theranostic approaches. However, encapsulation of hydrophilic imaging agents in the porous GPs is challenging. Here, we show that the unique coordination chemistry of Fe(III)-based macrocyclic T_1 MRI contrast agents permits facile encapsulation in GPs. Remarkably, the GPs labeled with the simple Fe(III) complexes are stable under physiologically relevant conditions, despite the absence of amphiphilic groups. In contrast to the free Fe(III) coordination complex, the labeled Fe(III)-GPs have lowered T_1 relaxivity and act as a silenced form of the contrast agent. Addition of a fluorescent tag to the Fe(III) complex produces a bimodal agent to further enable tracking of the nanoparticles and to monitor release. Treatment of the iron-labelled GPs with maltol chelator or with mildly acidic conditions releases the intact iron complex and restores enhanced T_1 relaxation of the water protons.

Introduction

Yeast derived β-glucan particles (GPs) are well-known vehicles for transport and delivery of a wide range of drugs with different physicochemical properties including charged macromolecules and lipophilic drugs.[1] These particles contain hollow shells that are prepared by using a series of chemical extractions of *Saccharomyces cerevisiae* following destruction of the yeast by heat. The GP are highly porous, and ellipsoidal in shape with approximate dimensions between 2-4 microns.[2] One advantage of using GPs as drug carriers is that β-1,3-D-glucan polymers, the major component of GPs, have dectin-1 receptor targeting properties. The dectin-1 receptor is expressed in several types of immune cells that play a key role in anti-fungal immunity. Thus, GPs are promising delivery vehicles for targeting immune cells including monocytes and macrophages, as blood-circulating cells of the immune system that have a crucial role in acute and chronic inflammation. Targeting of macrophages has potential for delivering drugs to sites of inflammation that are characteristic of disease states including cancer or atherosclerosis.[3,4]

In order to identify inflammation for diagnostic purposes, encapsulation of an imaging agent may permit tracking of the GP carrier. For example, dyes have been encapsulated in GPs to enable fluorescence imaging of the particles.[5, 6] There is also recent interest in using GPs as nature-inspired microcarriers for delivering MRI contrast agents that specifically target macrophages.[3, 5-8]

The delivery of both drugs and imaging agents would facilitate the development of theranostic applications of GPs. However, incorporation of low molecular weight drugs or imaging agents for delivery is complicated by the negative charge and porous nature of GPs. To circumvent the high porosity of the particles, the small molecules may be encapsulated into nanoparticles or liposomes first, and then loaded inside the GP.[5, 9, 10] Release of the liposome encapsulated dye is facilitated by heating the GPs.[7] Another method to promote successful entrapment is to add long hydrophobic alkyl chains on the dye or on the MRI contrast agent.[6] However, simpler systems that could deliver small molecule contrast agents without added hydrocarbon chains or without lipids have advantages, especially for triggered release in the absence of heat.

Our laboratory has produced high spin Fe(III) macrocyclic complexes that function as effective T_1 MRI contrast agents in vivo as potential alternatives to lanthanide agents.[11] The solution speciation and water interactions of the Fe(III) complex are distinctly different than those of typical Gd(III) agents, yet their relaxivity is competitive with standard Gd(III) contrast agents. The bound water in the Fe(III) macrocyclic complexes does not exchange rapidly on the NMR time scale, rather the complexes produce relaxivity through strong second-sphere interactions with water protons. Here we show that one of these complexes interacts so strongly with GPs; there is no need for an amphiphilic tail. Fe(TOB) and its bimodal analogue Fe(TOD) (Scheme 1) remain in the hydrated glucan particles without liposomes or chemical modification in an interaction that may involve coordination bonds or electrostatic interactions of the positively charged complex with the negatively charged β-glucan particles. Moreover, this interaction with the GPs is readily

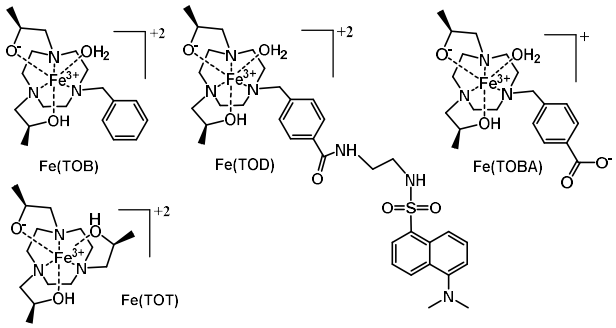

Scheme 1. Fe(III) complexes shown with predominate species at neutral pH.

reversed by treatment with mild acid or with a bidentate chelator to trigger the release the contrast agent. The goal of this study was to explore GPs as biocompatible delivery vehicles for T_1 Fe(III) based MRI contrast agents and to develop chemical triggers for the release of intact iron complexes.

Results and Discussion

Iron complexes and ternary interactions. Three Fe(III) macrocyclic complexes, Fe(TOB), Fe(TOD) and Fe(TOT), were chosen to study as contrast agents to encapsulate in GPs (Scheme 1). All three complexes are unusual examples of cationic contrast agents, whereas Gd(III) based T_1 MRI contrast agents are typically anionic or neutral.[12] The cationic nature of the complexes is supported by pH potentiometry studies of Fe(TOB) and Fe(TOT) complexes that are consistent with a single deprotonated hydroxypropyl pendent. The proposed form of the coordination complexes and their species at neutral pH are shown in Scheme 1.[11-13] These complexes are resistant towards dissociation in 100 mM acid, and in solutions containing 25 mM hydrogen carbonate and 0.4 mM hydrogen phosphate at neutral pH.[11, 13] Fe(TOD), which was prepared here as a bimodal agent, has similar solution properties. Fe(TOD) contains a fluorescent dansyl group to better visualize the encapsulation of the complex in yeast cell wall particles, and for future cell uptake studies. The macrocycle was synthesized by appending dansyl to the non-coordinating benzyl pendent, followed by alkylation of the macrocycle (Scheme S1). Fe(TOD) has an effective magnetic moment in solution of 5.73, similar to that reported for Fe(TOB), Fe(TOBA) and Fe(TOT) and consistent with high spin Fe(III) complexes.[11, 13] Moreover, most of the ^{1}H NMR resonances of these complexes are broadened into the baseline, consistent with strong relaxivity of the Fe(III) center.

The relaxivity (r_1 or r_2 in $mM^{-1}s^{-1}$) measured over the concentration range of 100 to 400 μM is given for Fe(TOB) in both neutral and acidic solutions in Table 1 and for other Fe(III) complexes at neutral pH. The T_1 relaxivity of Fe(TOD) is lower than that of Fe(TOB), and closer to that of a related complex which contains a carboxylate in the para-position, Fe(TOBA), shown in Scheme 1. The lowered relaxivity of the Fe(TOBA) complex compared to Fe(TOB) is not fully understood.[11] Differences in relaxivity may be due to an electronic effect on the benzyl group and Fe(III) center that modulates interactions with water protons, or possibly to subtle differences in speciation. Here too with Fe(TOD), the relaxivity is lowered, despite the larger size of the molecule that would normally be expected to produce increased r_1 relaxation rates due to longer rotational correlation times. The r_2 relaxivity values for the Fe(III) complexes are between 2-3 times greater than the r_1 values.

The pentadentate macrocyclic ligands of Fe(TOB) and Fe(TOD) leave an open coordinate site for water or for other ligands to form ternary complexes. This led us to search for a ligand that would bind sufficiently strongly to the available coordination sites to more easily trigger release of the macrocyclic Fe(III) complexes from GPs.[14-17] These ligands should ideally bind to the complex without removing the iron, but would allow us to sequester the contrast agent. Moreover, we searched for ligands that would produce a new electronic absorbance band in the visible region of the spectrum to monitor complex formation. UV-vis screening experiments were done with commercially available ligands which are known to bind the Fe(III) cation.[17-20] Our focus was on bidentate ligands that would form ternary complexes, presumably by replacing the water ligand and forming a seven-coordinate Fe(III) center.

Several bidentate ligands, when titrated into solutions of Fe(TOB), produced a new visible electronic absorbance which is characteristic of ligand to metal to charge transfer (LMCT) bands for Fe(III) complexes.[14, 15, 21] Within the group of bidentate ligands, ligands having β-hydroxyl ketones displayed promising binding characteristics. The broad CT band from 400-600 nm imparts a red color to the adduct solution (Figure S1). Catechol, deferiprone, and maltol were among those studied, but only maltol produced a suitably strong interaction as shown by UV-vis spectroscopy titrations (Figure S15, S16 and S1). Hinokitiol interaction with Fe(TOB) was strong enough to sequester iron out of the Fe(TOB) complex over time, whereas catechol appeared to only weakly bind to Fe(TOB) (Figure S18, S15). Deferiprone bound to Fe(TOB), but more weakly than did maltol (Figure S17, S2). In contrast, other bidentate chelators with oxygen donors including lactate, bis-phosphonate, salicylate, or phalate did not produce a new absorbance in the visible region (Figure S20-S23).

Titration of maltol into a solution of Fe(TOB) was fit to a 1:1 binding isotherm to give a dissociation constant of 5.5×10^{-5} (Fig S2). The absorbance of the adduct remained unchanged in solutions maintained at 37 °C with 25 mM hydrogen carbonate, 0.4 mM hydrogen phosphate at neutral pH, or in PBS buffer. There was no detectable dissociation promoted by 1 mM $ZnCl_2$ at pH 7.2 over 12 h (Fig S8). In contrast to Fe(TOB) alone which requires a sugar stabilizer, meglumine, to keep the complex in solution at high millimolar concentrations at pH 7.2,[11] the Fe(TOB) adduct with maltol has excellent solubility in water even at physiological pH. This suggests that maltol forms a strong ternary complex with Fe(TOB).

Table 1. Relaxivity values for Fe(III) complexes measured at 4.7 T, 20 mM HEPES pH 7.2, 100 mM NaCl at 37 °C.

Complex	μ_{eff} (BM)	r_1 $(s \cdot mM)^{-1}$ pH 7	r_2 $(s \cdot mM)^{-1}$ pH 7	r_1 $(s \cdot mM)^{-1}$ pH 4.5
Fe(TOB)[a]	5.90	2.30 ± 0.10	4.47 ± 1.07	1.54 ± 0.01
Fe(TOBA)[a]	5.60	1.70 ± 0.10	5.05 ± 0.48	
Fe(TOD)	5.73	1.55 ± 0.01	5.55 ± 0.11	
Fe(TOB):Maltol	6.03	2.52 ± 0.07	4.18 ± 0.35	
Fe(Maltol)$_3$	5.30	0.54 ± 0.01	0.81 ± 0.08	

[a] pH 7 data for Fe(TOB) and Fe(TOBA) taken from reference 10.
[b] with Meglumine.

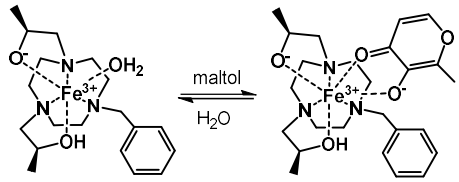

Scheme 2. Fe(TOB)-Maltol ternary complex

Several methods were used to further characterize the Fe(TOB)-maltol adduct. A high resolution ESI-FT-ICR mass spectrum of a solution with a 1:1 ratio of Fe(TOB) to maltol showed a peak for the Fe(TOB)(maltol) adduct (Fig S7). Moreover, a ^{1}H NMR titration of Fe(TOB) into a 5 mM solution of maltol at pH 7.2 showed the disappearance of the maltol proton resonances (Fig. S9). The disappearance of the maltol resonances are consistent with binding of maltol to a paramagnetic high spin Fe(III) center. Furthermore, if the maltol were to remove Fe(III) from Fe(TOB), the Fe(maltol)$_3$ complex would result. Synthesis of this complex and analysis by ^{1}H NMR spectroscopy shows two very broad proton resonances at 42 and 75 ppm (Fig S12), which is clearly not what we observe in maltol titrations of Fe(TOB) (Fig S13). Solutions of Fe(TOB)-maltol that were monitored for 12 h by ^{1}H NMR spectroscopy were unchanged over this time period, suggesting that the ternary adduct persisted. (Fig S14).

Other solution characterization included variable temperature ^{17}O NMR studies. There is little broadening of the ^{17}O NMR resonance in the presence of Fe(TOB)-maltol (Figure 2). This suggests that the adduct, like Fe(TOB), does not have a inner-sphere water ligand that exchanges rapidly on the NMR time scale.[11, 22] For comparison, Fe(DTPA) which lacks an inner-sphere water and Fe(CDTA) which has a bound water are shown. The ^{17}O NMR data for Fe(TOB) and Fe(TOB)(maltol) much more closely resemble that of Fe(DTPA) which lacks an inner-sphere water ligand.

Relaxivity measurements show a slight increase in r_1 relaxivity for the adduct compared to Fe(TOB) (Table 1). All in all, the data suggest that the maltol is bound strongly to the Fe(III) center as a bidentate ligand. Based on our data, we favour a ternary complex that has a directly bound maltol ligand, consistent with the observed LMCT band of the Fe(TOB)(maltol) adduct and the lack of maltol ^{1}H resonances observed in NMR titrations upon addition of Fe(TOB) (Fig S1, S3, S10). The maltol likely binds directly to the Fe(TOB) through displacement of water to give a seven coordinate complex (Scheme 2), analogous to a seven-coordinate Fe(III) macrocyclic complex reported recently.[23] While

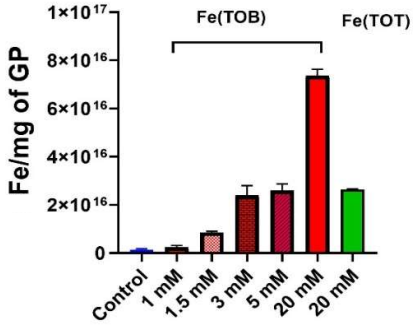

Figure 1. Total Fe content in (a) unlabeled, Fe(TOB) and Fe(TOT) labeled GP measured by ICP-MS. Mean ± SD is reported.

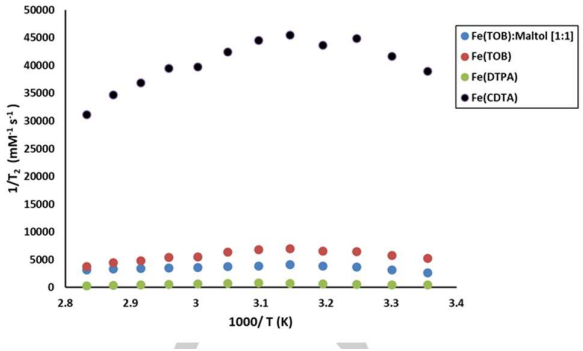

Figure 2. Comparison of 10 mM Fe(TOB):Maltol (1:1 equivalence), 10 mM Fe(TOB), 10 mM Fe(DTPA) and 10 mM Fe-CDTA ^{17}O NMR resonance broadening at pH 6.0 as a function of temperature. Fe(CDTA) was run at pH 5.6.

we do not know that exact nature of the coordination mode of maltol to Fe(TOB), it seems reasonable that the ligand would be bidentate. Consistent with this postulate, titration of Fe(TOT), a closed coordination complex, with maltol did not produce a UV-vis absorbance peak characteristic of a ternary complex (Figure S6). This comparison suggests that a displaceable water ligand on the Fe(III) complex is required for maltol binding.

Labeling and release of Fe(TOB) in glucan particles. The GPs were labelled by stirring the particles in an aqueous solution of Fe(TOB) for 16 h. The resulting particles were collected as a pellet and were visibly orange-brown in color due to Fe(TOB) loading (Figure S24). Fe(TOB) loading was found to be directly proportional to the concentration of iron complex in incubating solutions as shown by ICP-MS analysis of the labelled particles, (Figure 1). Moreover, a series of Z-spectra recorded on the Fe(TOB) labelled GPs also showed a correlation with Fe(TOB) labelling. In these experiments, a pre-saturation pulse is used to magnetically saturate protons that may chemically exchange with bulk water. The frequency of the pre-saturation pulse is varied to produce a plot of the water proton intensity (M_z/M_o) as a function of pre-saturation pulse frequency. Encapsulation of paramagnetic complexes into liposomes or cells produces broadened Z-spectra that are slightly asymmetric in shape. The asymmetry is attributed to the paramagnetic shift of the interior water protons and exchange of the protons to give a chemical exchange saturation (CEST) effect (Fig S25).[24, 25] We observed a broadened peak, consistent with increased T_2 effects from incorporation of the complex into the GP and a slight asymmetry characteristic of a CEST effect from magnetically shifted protons. The same broadened Z-spectra were observed even after 4 days of incubation in phosphate buffered saline at room temperature (Fig S26). This suggests the glucan particles are stable and will not release Fe(TOB) without an external stressor. Further experiments described below show that the water proton relaxivity of solutions containing the labelled GP did not change over time, supporting the robust nature of the Fe(TOB)-labelled GPs. SEM characterization showed mild morphology changes in the surface of the GP (Fig S29). The unlabeled GP appeared shrunken and dehydrated, but the labeled version was round, similar to literature reports of nanoparticle loaded GPs.[5]

For comparison, GPs were treated with Fe(TOT), as an example of a cationic complex that lacks water ligands and would not be expected to bind to the GPs through a coordination bond.

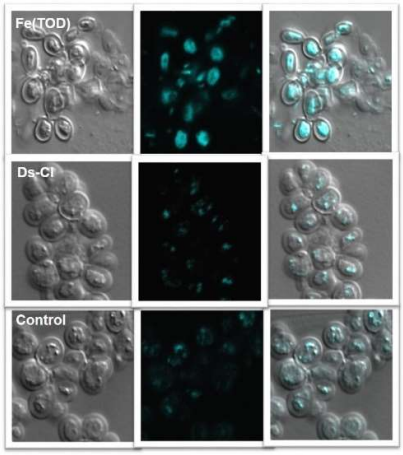

Figure 3. Fluorescence confocal microscopy images of glucan particles. (TOP) Fe(TOD) labeled GP (middle) Dansyl chloride labeled GP and (Bottom) Control GP. Excitation (405 nm) emission (520-560 nm). All examples show fluorescence with 5 μM scale.

However, this closed coordination complex might adhere to GPs due to cation charge of the complex. Fe(TOT) was indeed encapsulated in GPs, but only at a fraction (25%) of the amount of Fe(TOB) as shown in Figure 1 (right). This shows that the open coordination sphere of Fe(TOB) that permits binding to additional ligands also increases loading into GPs.

The Fe(TOD) complex was treated with GPs in order to utilize the fluorescent tag. The dansyl group of Fe(TOD) showed a fluorescence emission peak at 560 nm upon excitation at 340 nm (Figure S33). Confocal fluorescence microscopy of Fe(TOD) treated GPs suggests encapsulation of the Fe(TOD) complex in the GP (Figure 3). However, due to the long UV excitation of dansyl fluorophore, some auto fluorescence is observed in the control GP. In order to gauge the stability towards release of the Fe(III) complex in media, the labeled GPs were incubated in solution for 26 h and the fluorescence in solution was measured. (Figure S35). Between initial time points and 2 h, there was a small increase in fluorescence intensity, which we attribute to release of surface bound complex. However, from 2 h to 26 h there was little change in fluorescence intensity of the solution above the GPs, consistent with the robust nature of the Fe(TOD) labeled particles.

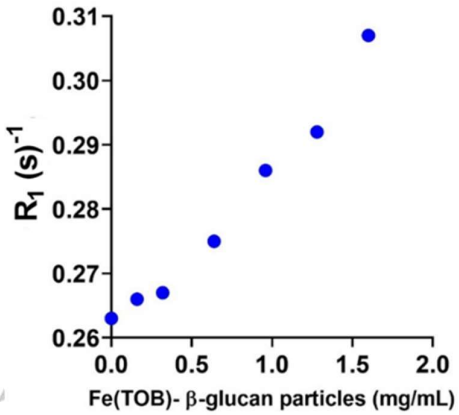

Figure 4. Relaxation rate constants of Fe(TOB) labeled GP suspended in collagen at 37 ºC in 4.7 T MRI scanner.

To further study the nature of small molecule dye interactions with GPs, we attempted to encapsulate dansyl alone or rhodamine-B in the GP. Interestingly, the dansyl dye could not be visualized upon treatment with GP by confocal microscopy. This suggests that either the dye was not encapsulated, or it passed through the large pores. By contrast, the cationic rhodamine-B dye was encapsulated and visualized in GPs by fluorescence microscopy (Figure S37), although the long exposure times we used suggested low dye loading. Time dependent studies suggested that rhodamine-B was partially released from the initial time points up to 2 h, which is attributed to loosely bound dye, perhaps at the surface. However, after 2 h, no further release was observed up to 24 h (Figure S36). Microscopy of the rhodamine-B loaded GPs also showed little leaching of the dye. This suggests that cationic dyes may be encapsulated into the GPs without liposomes or amphiphilic tails.

To study the potential of the Fe(TOB) loaded GP for MRI studies, R_1 rate constants were measured on labelled and unlabelled glucan particles suspended in collagen on a 4.7 Tesla MRI scanner (Figure S30). The R_1 relaxation rate constants for the Fe(TOB) labeled particles (3.03 ± 0.03 s^{-1}) were only marginally higher than the control GPs (3.45 ± 0.03 s^{-1}). The apparent quenching of R_1 relaxation rates of Fe(TOB) in GPs suggests a disruption of the second sphere water interaction which is the major contributor of the r_1 relaxivity of Fe(TOB).[11] In addition, the hydrophobic nature of the β-1,3-D-glucan polymer may inhibit water exchange. The increase in the R_1 relaxation rate constant for water protons in the sample, however, corresponds to the number of GPs per volume in a collagen matrix (Figure 4, Table S1). Dividing the relaxation rate constants by the iron content of the particles gave an r_1 of 0.21 $mM^{-1}s^{-1}$ (Figure S31). The r_2 relaxativity based on iron concentration was much higher (3.45 ± 0.27) $mM^{-1}s^{-1}$ which is expected from dominance of T_2 processes observed in paramagnetic particles at higher field strengths.[6] In comparison, Gd(III) labeled GPs have r_1 relaxivities of 22.3 $mM^{-1}s^{-1}$ at low magnetic fields (0.5 T), but r_1 decreases several fold at higher field strengths (7 T). Similarly, the r_2 values for the Gd(III) labeled GPs are an order of magnitude higher than r_1 at 7 T.[6] However, the Gd(III) labelled GPs have amphiphilic tails that anchor the complexes into the GPs. The Gd(III) complexes in these labeled GPs cannot be easily released. The goal in our studies, was to release the Fe(III) contrast agent.

Maltol treatment of the Fe(TOB) labeled GPs released the Fe(TOB) from the GPs as shown by Z-spectra and ICP-MS analysis of the yeast cell wall particles (Figure S27, Figure 5b). These studies show that essentially all of the Fe(TOB) was removed upon treatment with excess maltol after 3 h. Moreover, maltol treatment of Fe(TOB)-loaded GPs increased the R_1 rate constant for proton relaxation of the solution in contact with the particles (Figure 5a). Mildly acidic conditions (pH 4.5) also produced an increase in the proton relaxivity (Figure 5a). Acid triggered release of the Fe(III) complex bodes well for freeing the iron complexes in acidic phagosomes,[26-28] whereas maltol may provide a means of adding a chemical agent to trigger release.

The use of maltol as a triggering agent is promising based on its low toxicity in cell lines and in mice. For example, treatment with maltol is used to reduce nephrotoxicity, an off-target effect of cisplatin through reduction of oxidative stress, lipid peroxidation and apoptosis in HEK293 cell line.[29] The anti-inflammatory and anti-oxidant properties of maltol have been shown to prevent

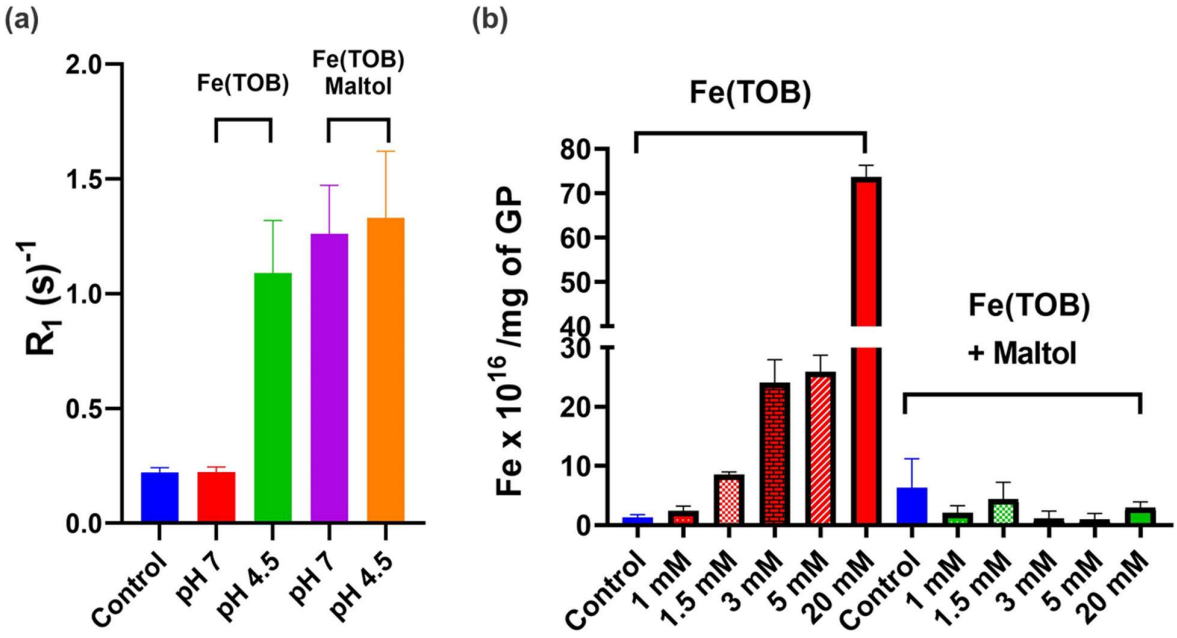

Figure 5.(a) R_1 relaxation rate constants for control GP-media and Fe(TOB) labeled GP-media at various pH values after 3 h incubation measured on a 9.4 T (400 MHz) NMR spectrometer. (b) Total Fe content in unlabeled and Fe(TOB) labelled GP (red) and total Fe content after 10 mM Maltol treatment for 3 h at 30 °C as measured by ICP-MS. Mean values are reported with ± 1% SD.

alcohol induced redox stress both in cell lines and in mice models even at high doses of 50-100 mg/kg.[30, 31] These studies are promising for the application of maltol as a chemical trigger to release Fe(TOB) from the glucan particles.

Conclusions

The unusual properties of cationic Fe(III) T_1 MRI contrast agents studied here facilitate labelling of GPs without further functionalization of the complexes or incorporation into liposomes as necessary for most dyes or contrast agents.[4,5,9] We propose that the cationic nature of the complexes enables this tight encapsulation in GPs, which are known to be negatively charged.[2, 5, 9] Further, Fe(TOB) shows higher loading than the Fe(TOT) complex suggesting additional coordination interactions with the GPs. The Fe(III) complex must be released from the GPs, however, to produce enhanced T_1 water proton relaxivity. As we show here, both mildly acidic conditions or a bidentate chelator trigger the release of the Fe(TOB) or the Fe(TOD) complex from the GPs.

The resistance of Fe(TOB) to acid and retention of r_1 relaxivity under acidic conditions makes Fe(TOB) an excellent candidate for imaging acidic vesicles found in cells such as macrophages.[27, 28] Thus, an enhanced MRI signal is anticipated upon maltol-mediated or acid mediated release of the Fe(III) complex. Conveniently, β-glucan particles selectively interact with dectin-1 receptors on the macrophages. This unique interaction has been extensively investigated in the literature for *in-vivo* and *ex-vivo* labelling of macrophages with drugs and imaging agents.[8, 10, 32, 33] Studies are underway to determine optimal conditions for the uptake and release of Fe(TOB) labeled particles in macrophages. [4, 34]

Experimental Section

Instrumentation. A Varian Inova 500 MHz NMR spectrometer equipped with FTS Systems TC-84 Kinetics Air Jet Temperature Controller was used to collect Z-spectra and ^{1}H NMR spectra. Fourier transform ion cyclotron resonance mass spectrometry (FT-ICR-MS) with 12T Bruker SolariXR 12 Hybrid was used to collect high resolution mass spectral data. Absorbance spectra were collected using a Beckman-Coulter DU 800 UV-vis Spectrophotometer equipped with a Peltier temperature controller. Fluorescence microscopy was done on Zeiss Axioplan2 microscope. T_1 imaging was performed on a 4.7 Tesla MRI scanner (ParaVision 3.0.2, Bruker Biospin, Billerica MA) with 35 mm Bruker single channel RF coil. Temperature was maintained at 37 °C during imaging using an MR-compatible heating system (SA Instruments, Stony Brook, NY). The concentration of Fe in yeast cell wall particles was determined by using Thermo X-Series 2 inductively coupled plasma mass spectrometry (ICP-MS). Confocal imaging was done on Lieca DMIR2 inverted fluorescence microscope equipped with a QImaging Retiga EXi CCD camera.

Materials. 3-Hydroxy-2-methyl-4*H*-pyran-4-one, 3-Hydroxy-1,2-dimethyl-4(1H)-pyridone, 5-(Dimethylamino)naphthalene-1-sulfonyl chloride and 4-(2-hydroxyethyl)-1-piperazineethanesulfonic acid (HEPES) buffer was purchased from Alfa Aesar. Nitric acid at 65-70% with greater than ≥99.999% purity (trace metals basis) was obtained from BeanTown Chemical. 100 ppm Fe standard solutions were purchased from Inorganic Ventures. Bovine collagen (3 mg/mL) was obtained from Advanced Biomatrix. [Fe(TOB)Cl]Cl and Fe(TOT)Cl_2 were prepared as reported.[11,41] The TOT ligand was synthesized according to a procedure reported in the literature.[35]

Binding of Maltol with Fe(TOB)

UV-Vis characterization. Solutions were prepared that contained 500 μM Fe(TOB) complex in 20 mM HEPES and 100 mM NaCl. A solution of maltol solution was added to the Fe(TOB) solution and monitored by using UV-vis spectroscopy. The change in absorbance at 480 nm was plotted against Fe(TOB) concentration in the cuvette to obtain the binding isotherms. The dissociation constants were determined by fitting the binding isotherms to binding models using graphpad prism 7.

For the kinetic inertness study, a 1:1 solution of 500 μM FeTOB and Maltol was prepared containing 20 mM HEPES and 100 mM NaCl. For extinction coefficient measurement 1:1 solution of FeTOB and Maltol was prepared at native pH. The stock solution was diluted to 3 different concentrations with 20 mM HEPES and 100 mM NaCl and UV-Vis response was observed. The change in absorbance at 480 nm was plotted against the adduct concentration. The resulting graph was fit to linear regression passing through the origin. The slope of the fit was used to obtain extinction coefficient in the 1 cm path length cuvettes.

Characterization of the Fe(TOB)-maltol adduct by NMR spectroscopy. Samples were prepared by dissolving 5 mM Maltol and 3.0 mM TMPS as an internal standard in D_2O and ^1H NMR spectra were recorded. For each experiment, Fe(TOB) was titrated into the maltol sample, the pH was adjusted to ~7.2 using NaOD and ^1H NMR spectra was recorded. All solutions were incubated for 10 min between the measurements. The average integration of paramagnetic peaks relative to the internal standard was used to determine the concentration of Fe(TOB)-Maltol adduct. For further NMR spectroscopy studies, a 1:1 solution of 10 mM FeTOB and Maltol was prepared and pH was adjusted to ~7.2. ^1H NMR spectra were recorded every 15 min to study the stability of the adduct.

Monitoring ternary Fe(TOB)-maltol adduct by UV-Vis spectroscopy. Samples were prepared by combining 500 μM Fe(TOB) complex and 500 μM Maltol. The absorbance peak at 482 nm was recorded over a period of 12 h at 37 °C. Control samples contained complex with 20 mM HEPES and 100 mM NaCl. For stability in PBS, samples were incubated in 1X PBS. The anion stability was determined in the presence of 0.40 mM hydrogen phosphate and 25 mM hydrogen carbonate solution at neutral pH. Solutions containing 1 mM HCl were used for acid stability studies. Zn(II) displacement assays contained 1 mM Zn(II) in 20 mM HEPES buffer and 100 mM NaCl.

^{17}O NMR measurements. Samples were prepared in water with 1% $H_2{}^{17}O$. The chemical shifts as well as the line width at half-height of the symmetric water peak were determined in the absence and in the presence of metal complex at variable temperatures at pH 7. The line width at half-height of the signal in absence and in presence of metal complex at variable temperatures was used to calculate the transverse relaxation times using Swift-Connick equations, as described in literature.[35] $1/T_2$ was calculated by subtracting the full width at half maximum (FWHM) of the ^{17}O resonance with Fe(III) complex from that in the absence of complex at pH 6.5.

T_1/T_2 Phantom Relaxivity measurements. Samples with variable concentrations (100, 200 and 400 μM) of 1:1 stoichiometric amounts of Fe(TOB) and Maltol in 20 mM HEPES, 100 mM NaCl and 35 g/L HSA at pH 7.4 were studied. T_1/T_2 relaxivity values were determined on a 4.7 Tesla MRI system as reported previously.[36] Briefly, T_1 relaxation rates of serial dilutions were measured using an inversion-recovery, balanced steady-state free precession (bSSFP) acquisition with the following parameters: TE/TR=1.5/3.0 ms, flip angle=30°, inv. repetition time=10 s, segments=8, frames=100. T_2 relaxation rates were measured using a multi-echo, Carr-Purcell-Meiboom-Gill (CPMG) sequence with a fixed TR of 4200 ms and TE times ranging from 20-1200 ms in 20 ms increments. The relaxation rate of each sample was calculated using non-linear regression analysis within MATLAB (MathWorks, Natick MA) and relaxivities were then calculated by linear regression (concentration vs. relaxation rate).

Glucan particles and Fe(TOB) labeling

Isolation of yeast glucan particles. Glucan particles were prepared as described.[3, 6, 7] Briefly, *Saccharomyces cerevisiae* of the *Sigma1278b* strain background was used.[37] The specific strain (PC538) is a typical wild-type (WT) strain with the following genotype: *MATa ste4 FUS1-HIS3 FUS1-lacZ ura3-52,*[38] and was used for all experiments in the study. Cells were grown for 3 days in 250 mL YEPD media to about 10 g. The cells were washed and resuspended in 1 M NaOH and heated for 1 h at 80 °C. The insoluble residue was collected by centrifugation at 4000 rpm for 15 min. To the pellet was added 1 M HCl to adjust the pH to <5. The resulting solution was heated at 55 °C for 1 h. The insoluble residue was again collected by centrifugation at 4000 rpm for 15 min. The resulting pellet was washed twice with isopropanol, acetone and ethanol respectively. The porous yeast cell wall particles were collected by centrifugation and allowed to dry for 16 h at 25 °C.

Fe(TOB) labeling of glucan particles. The glucan particles were hydrated for 16 h at 25 °C in 1X PBS. 10 mM FeTOB solution was prepared and added to the hydrated yeast cell wall particles. The solution was stirred at 25 °C for 1 h. The labeled particles were harvested by centrifugation followed by 3 washes in 1X PBS wash. The resulting labeled particles were suspended in 1X PBS for further studies.

Z-spectra measurements on Fe(TOB) labeled glucan particles. All samples were resuspended in 1X PBS for analysis. Z-spectra have been acquired in a range of ± 50ppm by acquiring a total of 101 data points (steps of 1 ppm) with B_1 = 12 μT at 37 °C.

Scanning Electron Microscopy (SEM) on glucan particles. Labeled and unlabeled glucan particles were concentrated by syringe filtration by a 0.2 micron Whatman nucleopore polycarbonate filter paper with 1 mL syringe (GE Whatman, catalog #889-78084, Maidstone, UK).[37] Cells were rinsed with buffer by syringe, treated with 100 % ethanol by syringe and incubated for 15 min. The filter paper was removed from the holder, placed in a petri dish and treated with hydroxymethyldiazane (HMDS). Samples were placed at 4 °C for 16 h and imaged the following day.

T_1 measurements of glucan particles and data analysis. Labeled and unlabeled glucan particles were washed three times with 1X PBS. The particles were resuspended in 3D collagen gel using the referenced protocol[39] in 5 mm borosilicate NMR sample tubes.[42] The relaxation rates of the particles were measured on 4.7 T animal MRI at 37 °C using the same protocol used for phantom measurements mentioned above. The relaxation rate of each sample was calculated using non-linear regression analysis in MATLAB.

Determination of Fe(TOB) loading in glucan particles. The concentration of Fe in the glucan particles was determined by inductively coupled plasma mass spectrometry (ICP-MS) (Thermo X-Series 2). After the internalization experiments, the glucan particles with and without Fe(TOB) complex were collected in 200 μL mili-Q (Milipore) water. Glucan solutions (100 μL) were digested with metal free nitric acid (900 μL) (65-70%). After digestion for 3 d, the samples were diluted to 2% HNO_3, 30 ppb cobalt standard solution was added in 10 mL mili-Q (Milipore) water and analyzed by ICP-MS. For internal standards, cobalt and indium standard solutions were used.

Statistical analysis. Results were expressed as mean value ± standard deviation (SD). Statistical analyses were performed using one-way ANOVA analysis followed by Tukey's multiple comparisons test by using GraphPad Prism 8. A P value of less than 0.005 was regarded as significant for cell uptake and viability studies, P value of less than 0.5 was regarded as significant for T_1 measurements on cells.

Procedure for synthesis of [Fe(TOD)]Cl_2.

N-(2-aminoethyl)-5-(dimethylamino)naphthalene-1-sulfonamide (1). The compound was synthesized according to a procedure reported in the literature.[40]

4-(bromomethyl)-N-(2-((5-(dimethylamino)naphthalene)-1-sulfonamido)ethyl)benzamide (2). 1-(4-(bromomethyl)phenyl)-2-chloroethan-1-one (0.28 mg, 0.95 mmol) was dissolved in THF and stirred at room temperature to form a homogenous solution. Compound (1) (0.22 mg, 0.95 mmol) was dissolved separately in THF and added slowly to the stirring solution. Immediate precipitation was observed upon addition. However, the reaction was stirred overnight till the solution turned clear. Solvent was removed under vacuum. The pure product was obtained using column chromatography with 20% MeOH in chloroform. The product was obtained as off-white powder in 60% yield. ^{1}H NMR (500 MHz, $CDCl_3$) δ 8.75 (1H, br), 8.38 (1H, br), 8.23 (1H, d, 10 Hz), 8.07 (1H, d, 10 Hz), 7.66 (2H, d, 10 Hz), 7.57 (3H, br, s), 7.51 (3H, br, s), 4.51 (2H, s), 3.53 (2H, t, 5 Hz), 3.17 (6H, s), 2.99 (2H, t, 5 Hz). ^{13}C NMR (75 MHz, CD_3OD) δ 167.8 (1C, s), 151.9 (1C, s), 142.5 (1C, s), 133.7 (1C, s), 130.6 (2C, s), 129.8 (2C, s), 129.2 (2C, s), 129.1 (1C, s), 128.6 (2C, s), 127.5 (2C, s), 127.4 (2C, s), 45.8 (2C, s), 43.3 (1C, s), 39.8 (1C, s), 32.3 (2C, s). FT-ICR-MS of $[C_{22}H_{24}BrN_3O_3S+H]^+$ calculated: 490.07945 found: 490.08010.

4-((4,7-bis((S)-2-hydroxypropyl)-1,4,7-triazonan-1-yl)methyl)-N-(2-((5-(dimethylamino)naphthalene)-1-sulfonamido)ethyl)benzamide (TOD). **Compound (3)** (0.10 mg, 0.50 mmol) was dissolved in ACN and stirred at room temperature. Compound (2) (0.28 mg, 0.56 mmol) was dissolved in acetonitrile separately and added slowly to the stirring solution. The solution was stirred at room temperature for 4 h. After 4 h the solution was centrifuged to remove salts and the supernatant was collected. Acetonitrile was removed from this solution under vacuum. A minimum amount of ethanol was added to the resultant solid to dissolve it. Diethyl ether was added to the solution to precipitate the product as a yellow sticky solid in 30% yield. ^{1}H NMR (500 MHz, CD_3OD) δ 8.50 (1H, t, 10 Hz), 8.39 (1H, d, 9Hz), 8.31 (1H, d, 10 Hz), 8.23 (2H, d, 10 Hz), 8.19 (1H, d, 5 Hz), 8.10 (1H, t, 10 Hz), 7.96 (2H, d, 5Hz), 7.71 (1H, t, 10 Hz), 7.52 (1H, d, 10 Hz), 7.50 (1H, d, 5 Hz), 3.54-3.47 (6H, br, s), 3.19-3.09 (6H, br, s), 2.86 (3H, s), 2.84 (2H, s), 2.80-2.70 (6H, m), 2.68-2.62 (6H, m), 1.13 (3H, s), 1.12 (3H, s). ^{13}C NMR (75 MHz, $CDCl_3$) δ 167.7 (1C, s), 135.0 (1C, s), 134.5 (1C, s), 133.0 (1C, s), 130.4 (2C, s), 129.7 (1C, s), 129.4 (1C, s), 129.0 (1C, s), 127.3 (2C, s), 116.4 (1C, s), 115.2 (1C, s), 63.67 (2C, s), 63.38 (1C, s), 58.31 (2C, s), 49.56 – 45.50 (6C, m), 45.33 (1C, s), 42.98 (1C, s), 39.88 (2C, s), 21.02 (2C, s). FT-ICR-MS of $[C_{29}H_{51}N_8O_7S + H]^+$ calculated: 655.35959 found: 655.35975.

[Fe(TOD)]Cl_2. TOD ligand (0.12 g, 0.17 mmol) was dissolved in ethanol. The mixture was stirred for 30 min and 5.0 mL ethanolic solution of $FeCl_2$ (0.035 g, 0.17 mmol) was added dropwise to the reaction mixture. No attempts were made to exclude O_2 in air from solutions. A precipitate was formed immediately upon addition of the $FeCl_2$ solution, but the reaction mixture was stirred overnight at room temperature. The precipitated complex was filtered and washed with diethyl ether (10 mL x 3). [Fe(TOD)]Cl_2 was collected as a yellow-orange solid with yields of 60%. Effective magnetic moment as measured by Evans method was 5.73. FT-ICR-MS of $[Fe(TOD)]^+$ calculated: 708.27796 found: 708.27508.

Fluorescence spectroscopy. Fe(TOD) samples were dissolved in 1X PBS with milli-Q water in 5 mm quartz cuvette. The samples were excited at the optimal wavelength for the dansyl fluorophore in the complex (Dansyl λ_{ex} = 340 nm).

Microscopy characterization. Yeast cells were washed three times in water before preparing the samples for imaging by fluorescence microscopy. Fluorescence imaging was done using RITC (Rhodamine Isothiocyanate) channel with exposure 1.5 s on a Zeiss Axioplan2 fluorescence microscope. For confocal microscopy the samples were added under an synthetic dextrose (SD) agar pad to avoid sample dehydration during the experiment.[41]

Maltol removal of Fe(TOB) bound to glucan particles. To the Fe(TOB) labeled glucan particles, 10 mM Maltol solution was added. The particles were incubated for 3 h at 25 ºC. After the incubation the particles were harvested through centrifugation followed by 3 times 1X PBS wash. Both supernatant and pellet was saved for ICP-MS analysis.

Z-spectra measurements on Fe(TOB) labeled glucan particles. All the samples were suspended in 1X PBS for the analysis. Z-spectra were acquired in a range of ± 50 ppm by acquiring a total of 101 data points (steps of 1 ppm) with B_1 = 12 μT at 37 ºC.

T_1 measurement on media. The Fe(TOB) labeled glucan particles were incubated in 1X PBS, acetate buffer pH 4.5, 10 mM Maltol in 1X PBS and 10 mM Maltol in acetate buffer at pH 4.5 at 37 ºC. Aliquots were taken at 3 h and 24 h, and media was collected through centrifugation. T_1 values of water protons were measure on Varian 400 MHz NMR spectrometer using an inversion-recovery pulse sequence.

Determination of Fe(TOB) loading in glucan particles using ICPMS. Concentration of Fe in the glucan particles was determined by using inductively coupled plasma mass spectrometry (ICP-MS) (Thermo X-Series 2). After the incubation, the glucan particles with and without Fe(TOB) followed by Maltol treatment were collected in 200 μL milli-Q (Millipore) water. GP solution (100 μL) were digested with metal free nitric acid (900 μL) (65-70%). After a three-day digestion process, the samples were diluted to 2% HNO_3, 30 ppb cobalt standard solution in 10 mL mili-Q (Milipore) water and analyzed by ICP-MS. Cobalt and indium standard solutions were used as internal standards.

Determination of dissociation of Fe(TOD) and rhodamine-B labeled glucan particles using Fluorescence spectroscopy. Fe(TOD) and rhodamine-B labeled glucan particles were incubated for 26 h at 37 ºC. 2 mM Maltol was added to all the samples after 24 h and incubated at 37 ºC for 2 h. The particles were centrifuged and aliquots were drawn from the supernatant at various time intervals for fluorescence spectroscopy. The Fe(TOD) samples were excited at λ_{ex} = 340 nm and Rhodamine-B samples were excited at λ_{ex} = 555 nm. The rhodamine-B labeled glucan particles were collected at the end for fluorescence microscopy.

Acknowledgements

JRM acknowledges the National Science Foundation (CHE-1710224). The authors would like to thank Chemistry Instrument Center (CIC), University at Buffalo. This work utilized ICP-MS and FTMS that was purchased with funding from a NSF Major Research Instrumentation Program (NSF CHE-0959565) and National Institutes of Health (S10 RR029517). The confocal imaging studies were funded by National Science Foundation Major Research Foundation grant # DBI 0923133. We thank Peter Bush for providing assistance with electron microscopy.

Keywords: Molecular imaging, β-glucan microparticles, biocompatible delivery, bimodal imaging agent, chelator mediated release, acid mediated release, targeted delivery, Imaging agent design.

[1] M. Chandana, D. Manasi, R. K. Jagat, K. S. Sanjeeb, *Curr. Drug Delivery* **2011**, *8*(1), 45-58.

[2] T. K. Upadhyay, N. Fatima, D. Sharma, V. Saravanakumar, R. Sharma. *EXCLI Journal* **2017,** *16*, 210-228.
[3] C. Cirizzi, W. Dastru, D. D. Castelli, V. Menchise, S. Aime, E. Terreno, *Curr. Mol. Imaging* **2015**, *4*(1), 29-34.
[4] K. R. Peterson, M. A. Cottam, A. J. Kennedy, A. H. Hasty, *Trends Pharmacol. Sci.* **2018**, *39*(6), 536-546.
[5] T. Ren, J. Gou, W. Sun, X. Tao, X. Tan, P. Wang, Y. Zhang, H. He, T. Yin, X. Tang, *Mol. Pharmaceutics* **2018**, *15*(7), 2870-2882.
[6] S. Figueiredo, J. N. Moreira, C. F. G. C. Geraldes, S. Rizzitelli, S. Aime, E. Terreno, *Chem. Commun.* **2011**, *47*(38), 10635-10637.
[7] F. Garello, R. Stefania, S. Aime, E. Terreno, D. Delli Castelli, *Mol. Pharmaceutics* **2014**, *11*(10), 3760-3765.
[8] E. R. Soto, A. C. Caras, L. C. Kut, M. K. Castle, G. R. Ostroff, *J. Drug Delivery* **2012**, *2012*, 13
[9] T. K. Upadhyay, N. Fatima, A. Sharma, D. Sharma, R. Sharma, *Artif. Cells, Nanomed., and Biotechnol.* **2019**, *47*(1), 427-435.
[10] M. Aouadi, G. J. Tesz, S. M. Nicoloro, M. Wang, M. Chouinard, E. Soto, G. R. Ostroff, M. P. Czech, *Nature* **2009**, *458*(7242), 1180-1184.
[11] E. M. Snyder, D. Asik, S. M. Abozeid, A. Burgio, G. Bateman, S. G. Turowski, J. Spernyak, J. R. Morrow, *Angew. Chem.., Int. Ed.*,**2020**, *132*(6), 2435-2440.
[12] J. Wahsner, E. M. Gale, A. Rodríguez-Rodríguez, P. Caravan, *Chem. Rev.* **2019**, *119*(2), 957-1057.
[13] D. Asik, R. Smolinski, S. M. Abozeid, T. B. Mitchell, J. A. Spernyak, J. R. Morrow, *Manuscript in preparation.*
[14] J. M. Harrington, S. Chittamuru, S. Dhungana, H. K. Jacobs, A. S. Gopalan, A. L. Crumbliss, *Inorg. Chem.* **2010**, *49*(18), 8208-8221.
[15] J. Li, V. Abbate, J. Jurach, G. Zhang, X. Kong, R. C. Hider, *ChemistrySelect* **2016**, *1*(2), 297-300.
[16] R. J. Abergel, K. N. Raymond, *Hemoglobin* **2011**, *35*(3), 276-290.
[17] A. S. Grillo, A. M. SantaMaria, M. D. Kafina, A. G. Cioffi, N. C. Huston, M. Han, Y. A. Seo, Y. Y. Yien, C. Nardone, A. V. Menon, J. Fan, D. C. Svoboda, J. B. Anderson, J. D. Hong, B. G. Nicolau, K. Subedi, A. A. Gewirth, M. Wessling-Resnick, J. Kim, B. H. Paw, M. D. Burke, *Science* **2017**, *356*(6338), 608-616.
[18] Z. D. Liu, R. C. Hider, *Coordination Chem. Rev.* **2002**, *232*(1), 151-171.
[19] Y.-S. Sohn, W. Breuer, A. Munnich, Z. I. Cabantchik, *Blood* **2008**, *111*(3), 1690-1699.
[20] A. Cilibrizzi, V. Abbate, Y.-L. Chen, Y. Ma, T. Zhou, R. C. Hider, *Chem. Rev.* **2018**, *118*(16), 7657-7701.
[21] K. H. Thompson, C. A. Barta, C. Orvig, *Chemical Society Reviews* **2006**, *35*(6), 545-556.
[22] E. M. Gale, J. Zhu, P. Caravan, *J. Am. Chem. Soc.* **2013**, *135*(49), 18600-18608.
[23] C. J.Bond, G. E. Sokolow, M. R. Crawley, P. J. Burns, J. M. Cox, R. Mayilmurugan, J. R. Morrow, *Inorg. Chem.* **2019**, *58*(13), 8710-8719.
[24] G. Mulas, G. Ferrauto, W. Dastrù, R. Anedda, S. Aime, E. Terreno, *Mag. Reson. Med.* **2015**, *74*(2), 468-473.
[25] E. Terreno, S. Geninatti Crich, S. Belfiore, L. Biancone, C. Cabella, G. Esposito, A. D. Manazza, S. Aime, *Mag. Reson. Med.* **2006**, *55*(3), 491-497.
[26] D. Hirayama, T. Iida, H. Nakase, *Int. J. mol. sci.* **2017**, *19*(1), 92.
[27] D. G. Russell, B. C. Vanderven, S. Glennie, H. Mwandumba, R. S. Heyderman, *Nat Rev Immunol* **2009**, *9*(8), 594-600.
[28] Y. K. Oh, R. M. Straubinger, *Infec. Immun.* **1996**, *64*(1), 319-325.
[29] X.-J. Mi, J.-G. Hou, Z. Wang, Y. Han, S. Ren, J.-N. Hu, C. Chen, W. Li, *Sci. rep.* **2018**, *8*(1), 15922-15922.
[30] Y. X. Han, Q.; Hu, J.-N.; Han, X.-Y.; Li, W.; Zhao, L.-C. , *Nutrients* **2015**, *7*, 682-696.
[31] W. W. Liu, Z.; Hou, J.-G.; Zhou, Y.-D.; He, Y.-F.; Jiang, S.; Wang, Y.-P.; Ren, S.; Li, W., *Molecules* **2018**, *23*, 2120.
[32] S. Figueiredo, J. C. Cutrin, S. Rizzitelli, E. De Luca, J. N. Moreira, C. F. G. C. Geraldes, S. Aime, E. Terreno, *Mol. Imaging Biol.* **2013**, *15*(3), 307-315.
[33] F. Garello, F. Arena, J. C. Cutrin, G. Esposito, L. D'Angeli, F. Cesano, M. Filippi, S. Figueiredo, E. Terreno, *RSC Adv.* **2015**, *5*(43), 34078-34087.
[34] Y. Pei, Y. Yeo, *J. Controlled Release* **2016**, *240*, 202-211.
[35] S. M. Abozeid, E. M. Snyder, T. Y. Tittiris, C. M. Steuerwald, A. Y. Nazarenko, J. R. Morrow, *Inorg. Chem.* **2018**, *57*(4), 2085-2095.
[36] S. J. Dorazio, P. B. Tsitovich, K. E. Siters, J. A. Spernyak, J. R. Morrow, *J. Am. Chem. Soc.* **2011**, *133*(36), 14154-14156.
[37] C. J. Gimeno, P. O. Ljungdahl, C. A. Styles, G. R. Fink, *Cell* **1992**, *68*(6), 1077-1090.
[38] J. Chow, M. Notaro, A. Prabhakar, S. J. Free, P. J. Cullen, *J. Fungi.* **2018**, *4*(3), 93-110.
[39] Y. Farhat, *The Protocol Place.* September 2012. Accessed on 03/08/2019. <http://protocol-place.com/>
[40] C. Blaszykowski, S. Sheikh, P. Benvenuto, M. Thompson, *Langmuir* **2012**, *28*(5), 2318-2322.
[41] D. T. Daniel R. Rines, Jonas F. Dorn, Paul Goodwin, and Peter K. Sorger, *Cold Spring Harb Protoc* **2011**, *9*, 1026-1041.
[42] A. Patel, D. Asik, J. A. Spernyak, P. J. Cullen, J. R. Morrow, *Journal of Inorganic Biochemistry* **2019**, *201*, 110832.

10.1002/cmdc.202000003

WILEY-VCH

FULL PAPER

Entry for the Table of Contents

Insert graphic for Table of Contents here. ((Please ensure your graphic is in **one** of following formats))

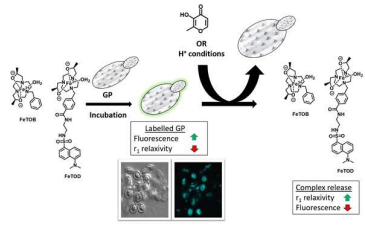

Yeast derived β-glucan particles (GPs) are effective microcarriers for targeting immune system cells, but the porosity of the GPs makes it challenging to load small molecule drugs or imaging agents. Here we show that members of a new class of cationic Fe(III)-based MRI contrast agent are encapsulated in the GPs in a stable form. Release of contrast agent produces increased T_1 proton relaxation as triggered by mild acid or a bidentate chelator.

Institute and/or researcher Twitter usernames: ((optional))